ably a similar ligand arrangement in the acyl–hydride complexes **6**, could account for the stability of these derivatives. Another reasonable explanation is that for aldehyde elimination to be facilitated or for hydride migration to the carbene ligand to occur, the hydride and organic ligands must be simultaneously attached to the same metal at some point in the reaction. Migration of hydride to W appears more reasonable than carbene or acyl migration to Ir, but there is apparently no tendency for either of these to occur. The W center in these derivatives is coordinatively saturated and hydride migration apparently cannot occur without ligand loss on W. The crystal structure of **2** in which the hydride was located and refined clearly shows that the hydride is terminally bound to Ir with no interaction with W.

It is significant that even though interesting acyl, carbene, and hydride ligands can be separately placed on the W and Ir centers in **2** and its derivatives, these ligands steadfastly refuse to interact even under forcing conditions. As noted above this may be due to the relative inertness of the third-row metals in these complexes and/or due to the steric constraints imposed by the two phosphido bridges. It is also interesting to note that none of these ligands in **2**, **6**, and **7** interact simultaneously with both metals even though bridging structures such as **13**, **14**, and **15** do not appear unreasonable on any obvious grounds.

Future work in this program will focus on complexes containing more reactive first- and second-row metals as well as further studies of compounds possessing only one sterically demanding phosphido bridge.

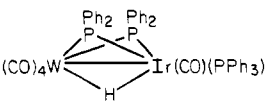

13

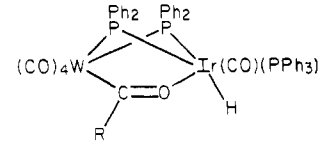

14

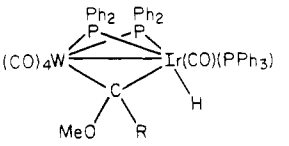

15

Acknowledgment. This work was supported in part by the Department of Energy, Office of Basic Energy Sciences. G.L.G. gratefully acknowledges the Camille and Henry Dreyfus Foundation for a Teacher–Scholar Award (1978–1983), the John Simon Guggenheim Memorial Foundation for a fellowship (1982–1983), the SOHIO and Union Carbide Corporations for grants which contribute to this research, and Johnson-Matthey Inc. for a loan of Ir salts.

Supplementary Material Available: Listings of anisotropic temperature factors, structure factors, and bond angles (63 pages). Ordering information is given on any current masthead page.

X-ray Crystal Structure for Two Disilenes

Mark J. Fink, Michael J. Michalczyk, Kenneth J. Haller, Robert West,* and Josef Michl‡

Departments of Chemistry, University of Wisconsin, Madison, Wisconsin 53706, and University of Utah, Salt Lake City, Utah 84112

Received November 28, 1983

The synthesis and X-ray crystal structures of tetramesityldisilene, **1a**, and *trans*-1,2-di-*tert*-butyl-1,2-dimesityldisilene, **1b**, are reported. The silicon–silicon bond lengths, 216.0 pm for **1a** and 214.3 pm for **1b**, are consistent with silicon–silicon double bonding in these molecules. The two silicon atoms and four attached carbons in **1b** are coplanar, but **1a** has a distorted structure with moderate anti pyramidalization at the silicon atoms. The differences in molecular geometry and the question of aryl–silicon conjugation are discussed. Crystals of **1a** are tetragonal of space group $I4_1/a$; crystals of **1b** are triclinic of space group $P\bar{1}$.

Following the recent synthesis of kinetically stable compounds with silicon–carbon[1] and silicon–silicon double bonds,[2] a structural chemistry of tricoordinate silicon is beginning to emerge.[3,4] The disilenes, as silicon counterparts of olefins, have attracted the attention of chemists for over 60 years.[5] These long sought species were proposed in 1968 as transient species in the pyrolysis of disilabicyclooctadienes,[6] and since that time considerable evidence has been presented for disilenes as reaction intermediates.[5,7] The first stable disilene, tetramesityldisilene, was synthesized in 1981 by photolysis of a polysilane precursor.[2a] The stability of this compound is attributed to the prevention of bimolecular condensations by the sterically large mesityl rings. This and other similar molecules have been subsequently synthesized by our group and others with use of a variety of methods.[2]

The spectroscopic properties and chemical reactivity of tetramesityldisilene are characteristic of a genuinely doubly bonded compound. The σ–π nature of the silicon–silicon

‡ J.M., University of Utah. M.J.F., M.J.M., K.J.H., and R.W., University of Wisconsin.

(1) Brook, A. G.; Abdesaken, F.; Gutekunst, B.; Gutekunst, G.; Kallury, R. K. *Chem. Commun.* **1981**, 191.

(2) (a) West, R.; Fink, M. J.; Michl, J. *Science (Washington, DC)* **1981**, *214*, 1343. (b) Boudjouk, P.; Han B.-H.; Anderson, K. R. *J. Am. Chem. Soc.* **1982**, *104*, 4992. (c) Masamune, S.; Hanazawa, Y.; Murakami, S.; Bally, T.; Blount, J. F. *Ibid.* **1982**, *104*, 1150. (d) Watanabe, H.; Okawa, T.; Kato, M.; Nagai, Y. *Chem. Commun.* **1983**, 781. (e) Michalczyk, M. J.; West, R.; Michl, J. *J. Am. Chem. Soc.*, in press. (f) Masamune, S.; Murakami, S.; Tobita, H. *Organometallics* **1983**, *2*, 1464.

(3) Brook, A. G.; Nyburg, S. C.; Abdesaken, F.; Gutekunst, B.; Gutekunst, G.; Kallury, R. K. M. R.; Poon, Y. C.; Chang, Y. M.; Wong-Ng, W. *J. Am. Chem. Soc.* **1982**, *104*, 5667.

(4) Fink, M. J.; Michalczyk, M. J.; Haller, K. J.; West, R.; Michl, J. *Chem. Commun.* **1983**, 1010.

(5) Gusel'nikov, L. E.; Nametkin, N. S. *Chem. Rev.* **1979**, *79*, 530.

(6) (a) Peddle, G. J. D.; Roark, D. N.; Good, A. M.; McGeachin, S. G. *J. Am. Chem. Soc.* **1969**, *91*, 2807; (b) Roark, D. N.; Peddle, G. J. D. *Ibid.* **1972**, *94*, 161.

(7) West, R. *Pure Appl. Chem.* **1984**, *00*, 000.

0276-7333/84/2303-0793$01.50/0

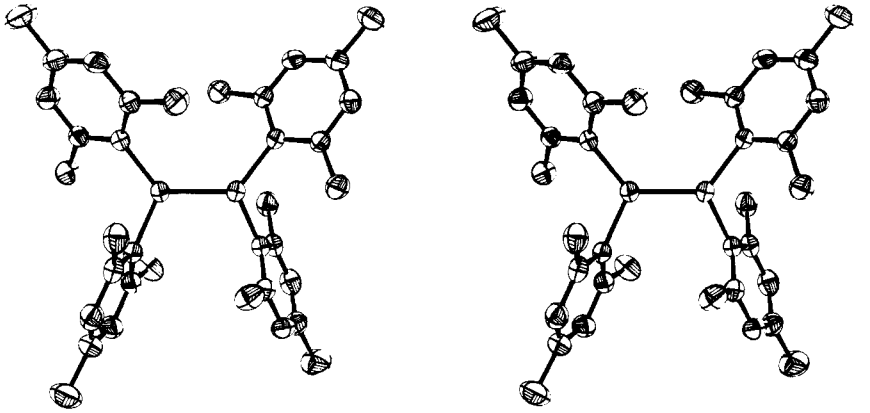

Figure 1. Stereoscopic ORTEP drawing of **1a**. Atoms are represented by their 50% probability ellipsoids.

Scheme I

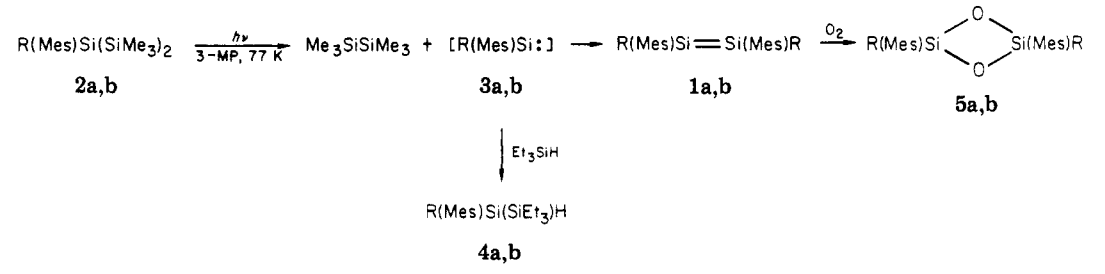

a, R = mesityl; b, R = CMe_3

bond is manifested by a $\pi \rightarrow \pi^*$ transition in the visible region[8] as well as by a large anistropy of the ^{29}Si chemical shift tensor.[9] Representative chemical reactions include the addition of alcohols and alkynes across the π bond.[10] In a preliminary account, we reported the X-ray crystal structure of **1a**.[4] The short silicon–silicon bond length (216.0 pm) found for **1a** is also consistent with the double-bond formalism. The disilene framework in this compound is not coplanar; the silicon atoms are moderately anti pyramidalized. In this paper we report the synthesis and solid-state structure of **1a** and of a related compound, *trans*-1,2-di-*tert*-butyl-1,2-dimesityldisilene (**1b**)—a molecule with a planar geometry in the solid state.

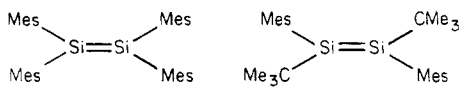

1a **1b**

Me = CH_3; Mes = mesityl (2,4,6-trimethylphenyl)

Synthesis

Photolysis of the trisilanes **2a** and **2b** at 254 nm in pentane or other alkane solvents gave yellow solutions containing the disilenes **1a** and **1b**. Progress of the reactions was followed by GLC (see Experimental Section). The photolysis can be carried out successfully at room temperature, but optimum yields of disilenes were obtained when the photolysis was performed at −50 to −100 °C where the disilene products precipitate. By GLC or NMR analysis the yield of disilene under these conditions is >95%. Separation of the solid product and recrystallization from pentane at −78 °C gave analytically pure disilenes.

Photolysis of the trisilanes **2a** and **2b** in 3-methylpentane glasses (3-MP) at 77 C produced highly colored species identified as the silylenes **3a** (blue) and **3b** (red).[11] The assignment of these species as silylenes was confirmed by warming of 3-MP glasses which contained both the colored species and an excess of the silylene trap, triethylsilane.[12] Under these conditions, the trapped products **4a** and **4b** were obtained quantitatively. In the absence of trapping agents, melting of the colored 3-MP glasses gave disilene products as shown in Scheme I.

Although silylenes have been demonstrated to dimerize in the gas phase,[13] we believe that these are the first unambiguous examples of silylene dimerization in solution. It is interesting that only the less hindered trans isomer of **4** is formed from **3b**, suggesting that steric factors are of great importance in the dimerization of silylenes.

Pure **1a** is a bright yellow and **1b**, a pale yellow, crystalline solid. Disilene **1a** is strongly thermochromic, turning from yellow to orange and eventually red when heated and melting at 178 °C to a red liquid. The color changes are reversible if the melt is cooled promptly, but decomposition takes place within minutes above 178 °C. Compound **1b** does not show thermochromism when heated but does become nearly colorless when chilled to 77 K. It is even more stable than **1a**, surviving heating to 225 °C, well above its melting point of 165–173 °C.

Although both **1a** and **1b** react with atmospheric oxygen to give cyclodisiloxanes **5a,b** (Scheme I), their reactivities toward oxygen (in benzene solution) differ significantly, with **1a** being much more reactive. A similar difference is also observed between the two solids. Powdered samples of **1a** are oxidized completely within a few minutes when

(8) Fink, M. J.; Michalczyk, M. J.; De Young, D. J.; West, R.; Michl, J., unpublished research.
(9) Zilm, K. W.; Grant, D. M.; Michl, J.; Fink, M. J.; West, R. *Organometallics* **1983**, *2*, 193.
(10) Fink, M. J.; De Young, D. J.; West, R.; Michl, J. *J. Am. Chem. Soc.* **1983**, *105*, 1070.
(11) The color of these species is attributed to a low-energy n → p transition largely localized on the silicon atom. See: Drahnak, T. J.; Michl, J.; West, R. *J. Am. Chem. Soc.* **1979**, *101*, 5427.
(12) Gaspar, P. P. In "Reactive *Intermediates*"; Jones, M., Jr., Moss, R. A., Eds.; Wiley: New York, 1978; p 229.
(13) Nakadaira, Y.; Kobayashi, T.; Otsuka, T.; Sakurai, H. *J. Am. Chem. Soc.* **1979**, *101*, 486.

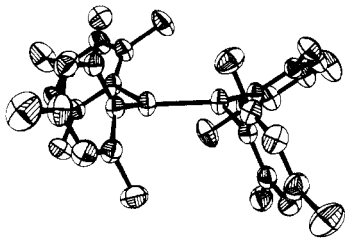

Figure 2. ORTEP drawing of **1a** showing the pyramidalization about the silicon rings.

Table I. Interatomic Distances (pm) in 1a (esd's in Parentheses)

Si-Si	216.0 (1)	C(16)-C(19)	151.8 (4)
Si-C(11)	188.0 (2)	C(21)-C(22)	141.6 (3)
Si-C(21)	187.1 (2)	C(21)-C(26)	141.6 (3)
C(11)-C(12)	140.6 (3)	C(22)-C(23)	138.6 (3)
C(11)-C(16)	140.8 (3)	C(22)-C(27)	150.9 (4)
C(12)-C(17)	151.9 (4)	C(23)-C(24)	138.6 (4)
C(12)-C(13)	139.0 (3)	C(24)-C(28)	151.1 (4)
C(13)-C(14)	137.7 (4)	C(24)-C(25)	137.7 (4)
C(14)-C(15)	139.0 (4)	C(25)-C(26)	138.6 (3)
C(14)-C(18)	150.9 (4)	C(26)-C(29)	150.8 (3)
C(15)-C(16)	137.8 (4)		

exposed to air. Similar samples of **1b** oxidize only over the span of a few hours, enabling the manipulation of **1b** in air for brief periods. The difference in reactivity may result from the greater steric shielding provided by *tert*-butyl groups compared to mesityl groups.

Structure of Tetramesityldisilene (1a). Figure 1 is a stereoscopic ORTEP drawing of tetramesityldisilene in the crystal. The molecule possesses a twofold rotation axis which in Figure 1 lies in the plane of the paper and passes through the silicon–silicon bond. The four aryl substituents are disposed about the silicon–silicon framework in a roughly helical fashion in which two of the cis related rings are more nearly coplanar with the silicon–silicon bond axis.

The two silicons and four pendant carbons deviate from planarity. The distortion can be described as a moderate anti pyramidalization of the silicons and a slight twisting along the silicon–silicon bond axis. The trans bent geometry of the disilene framework in **1a** is seen clearly in the ORTEP drawing of Figure 2. The degree of pyramidalization at the silicon can be gauged by the 18° angle formed by the C_{aryl}–Si–C_{aryl} plane and the silicon–silicon bond axis.

The torsional distortion along the silicon–silicon axis results in a twist angle of 6.5 (1)°, as illustrated in the Newman projection in Figure 3. The twist angle in this case is taken as half the difference of the angles subtended by the C(11)–Si–Si″ and C(11′)–Si–Si′ planes [29.5 (2)°] and the C(21)–Si–Si, and C(21′)–Si–Si′ planes [16.4 (2)°]. (The numbering schemes for **1a** and **1b** are shown in Figure 4.)

One pair of cis-related mesityl rings is in an orientation more nearly in the plane of the silicon–silicon bond than the other pair. The mean planes of this set of aromatic rings form angles of 35° with the Si–Si′–C_{aryl} plane whereas the other set forms an analogous angle of 78°. The two sets of rings are nearly orthogonal to each other, the angle formed by the intersection of the mean planes of geminal rings being 85°.

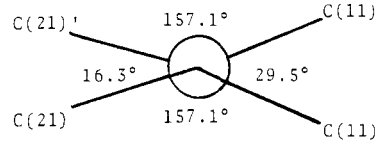

Figure 3. Newman projection of **1a** along the Si–Si axis showing the twist angles. The numbering scheme is shown in Figure 4; Si′ is in back of Si.

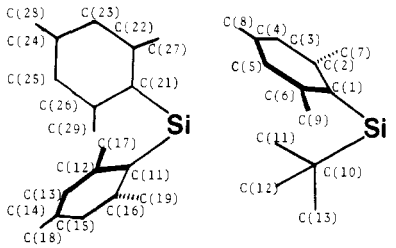

Figure 4. Numbering schemes for **1a** and **1b** (see Figures 1 and 6 for structural details).

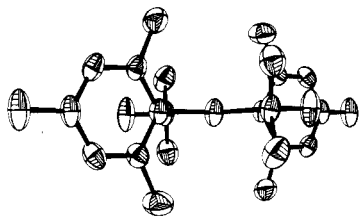

Figure 5. ORTEP drawing depicting a Newman projection of **1b**. The Si–Si axis is perpendicular to the plane of the paper. Atoms are represented by their 50% probability ellipsoids.

A most significant feature of this molecule is the short silicon–silicon bond length of 216.0 pm. The independent silicon–carbon bond lengths are 187 and 188 pm. The carbon–carbon bond lengths in the mesityl rings are normal; the endocyclic distances range from 138 to 142 pm, and the exocyclic distances span 151–152 pm. Other bond lengths and angles for **1a** are listed in Tables I and II.

Structure of 1b. Molecules of **1b** possess a center of symmetry midway between the two silicons. The structure differs from **1a** in that the silicon–carbon framework in the 1b molecule is planar. This is best illustrated by the Newman projection depicted in the ORTEP drawing of Figure 5. The mesityl rings in this molecule are skewed nearly orthogonal to the disilene framework, a feature best appreciated in the stereoscopic ORTEP illustration of Figure 6. The angle subtended by the mesityl rings and the framework plane is 88°.

The silicon–silicon bond length is 214.3 pm, slightly shorter than found for **1a**. The silicon–carbon bond distances to the *tert*-butyl and mesityl groups are 190 and

Table II. Interatomic Angles (deg) in 1a (esd's in Parentheses)

Si-Si-C(11)	113.9 (1)	C(13)-C(14)-C(18)	121.5 (3)	C(21)-C(22)-C(27)	122.3 (2)
Si-Si-C(21)	126.8 (1)	C(15)-C(14)-C(18)	120.4 (3)	C(23)-C(22)-C(27)	118.2 (2)
Si-C(11)-C(12)	122.5 (2)	C(14)-C(15)-C(16)	121.6 (2)	C(22)-C(23)-C(24)	122.6 (2)
Si-C(11)-C(16)	119.4 (2)	C(11)-C(16)-C(15)	120.4 (2)	C(23)-C(24)-C(25)	117.5 (2)
C(12)-C(11)-C(16)	118.1 (2)	C(11)-C(16)-C(19)	121.1 (2)	C(23)-C(24)-C(28)	121.8 (3)
C(11)-C(12)-C(13)	119.8 (2)	C(15)-C(16)-C(19)	118.4 (2)	C(25)-C(24)-C(28)	120.8 (3)
C(11)-C(12)-C(17)	122.1 (2)	Si-C(21)-C(22)	124.6 (2)	C(24)-C(25)-C(26)	122.7 (2)
C(13)-C(12)-C(17)	118.1 (2)	Si-C(21)-C(26)	117.3 (2)	C(21)-C(26)-C(25)	119.7 (2)
C(12)-C(13)-C(14)	122.0 (3)	C(22)-C(21)-C(26)	118.1 (2)	C(21)-C(26)-C(29)	121.7 (2)
C(13)-C(14)-C(15)	118.1 (2)	C(21)-C(22)-C(23)	119.5 (2)	C(25)-C(26)-C(29)	118.6 (2)

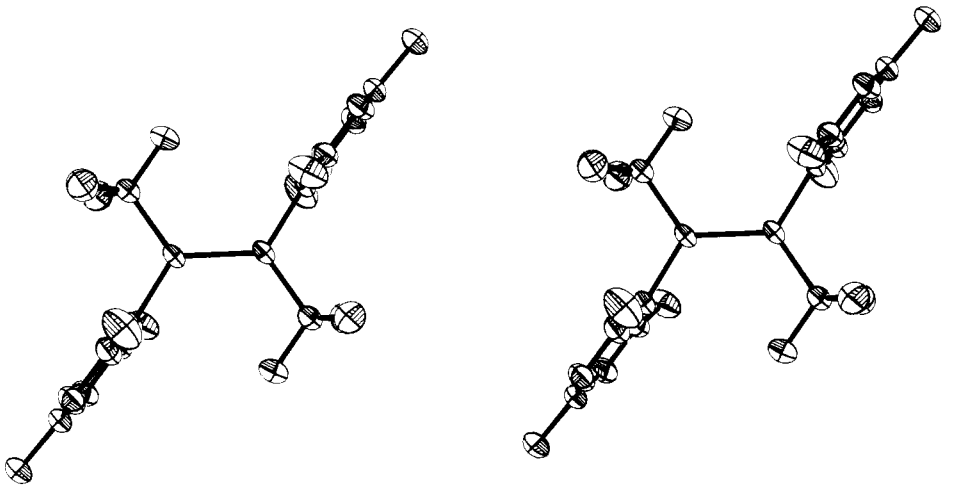

Figure 6. Stereoscopic ORTEP drawing of **1b** showing the orientation of the mesityl rings to the disilene framework.

Table III. Interatomic Distances in 1b (esd's in Parentheses)

Si-Si	2.143 (1)	C(4)-C(5)	1.377 (4)
Si-C(1)	1.884 (2)	C(4)-C(8)	1.514 (3)
Si-C(10)	1.904 (3)	C(5)-C(6)	1.396 (3)
C(1)-C(2)	1.405 (3)	C(6)-C(9)	1.508 (4)
C(1)-C(6)	1.413 (3)	C(10)-C(11)	1.528 (3)
C(2)-C(3)	1.397 (3)	C(10)-C(12)	1.542 (4)
C(2)-C(7)	1.506 (4)	C(10)-C(13)	1.526 (4)
C(3)-C(4)	1.374 (4)		

188 pm, respectively. Other bond lengths and angles for **1b** are given in Tables III and IV.

Bond Lengths

The silicon–silicon bond lengths for **1a** and **1b** are significantly shorter than a typical silicon–silicon single bond distance, consistent with the high bond order for the disilenes. For example, the silicon–silicon bond length in **1a** is 19–20 pm shorter than that of tetramesityldisilane (**6**) which has two independent distances of 235.0 and 236.2 pm.[14] The magnitude of bond length contraction is slightly greater than that found in going from a carbon–carbon single bond to a carbon–carbon double bond: compare tetraphenylethane (154 pm)[15] and tetraphenylethylene (135.5 pm).[16] On a percentage basis the bond contraction found for the silicon compounds, 8–9%, is a little less than for carbon (~12%). This indicates that the two disilenes have a strong π bonding component, although probably weaker than that in olefins. The observation is consistent with a number of theoretical studies which place the π bond strength of Si_2H_4 at roughly 30 kcal/mol,[17] about half the π bond strength for ethylene.

The weaker π bonding in disilenes relative to olefins is generally attributed to the less efficient overlap of the 3p orbitals on silicon.[2a] Similar overlap is expected to be even poorer for the 4p or 5p orbitals of the germanium and tin analogues of olefins. The strongly anti-pyramidalized structure of the distannene **7** may result from the ineffectiveness of pπ–pπ bonding in these systems: the tin–tin distance in **7** is identical with that of the tin–tin single bond in hexaphenyldistannane (**8**).[18]

Theoretical calculations of the silicon–silicon bond length in Si_2H_4 center about 215 pm[17,19] in good agreement with the observed bond lengths in **1a** and **1b**. The presence of bulky substituents apparently has no large effect on the silicon–silicon distances in these systems. Brook has previously noted that similar covalent radii for sp^2–π silicon can be obtained either from the disilene **1a** (108 pm) or from the silene **9** (109 pm);[3] the silicon covalent radius from **1b** is 107 pm. It is interesting that the covalent radius of silicon calculated from the silene **9** is slightly larger than that from the two disilenes, opposite to what is predicted by the Schomaker–Stevenson relation. The silicon–carbon double bond in **9** may be lengthened by resonance interaction with the adjacent oxygen of the siloxy group.[3]

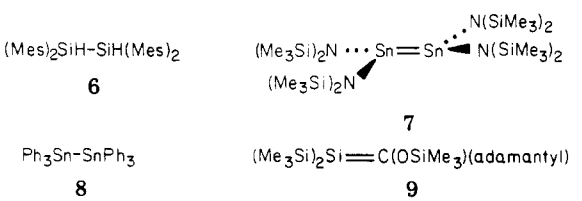

Molecular Geometries

The differences in the molecular geometries of **1a** and **1b** in the solid state are striking. The distortions of the double bond in **1a**, bond twisting and pyramidalization, are sometimes seen in olefins which have extremely bulky substituents.[20] and so presumably are associated with steric effects; but **1b**, which should be at least as hindered as **1a**, does not show these distortions.[21]

(14) Baxter, S. G.; Mislow, K.; Blount, J. F. *Tetrahedron* **1980**, *36*, 605.
(15) Dougherty, D. A.; Mislow, K.; Blount, J. F.; Wooten, J. B.; Jacobus, J. *J. Am. Chem. Soc.* **1977**, *99*, 6149.
(16) Hoekstra, A.; Vos, A. *Acta Crystallogr., Sect. B* **1975**, *B31*, 1722.
(17) (a) Daudel, R.; Kari, R. E.; Poirier, R. A.; Goddard, J. D.; Csizmadia, I. G. *J. Mol. Struct.* **1978**, *50*, 115. (b) Poirier, R. A.; Goddard, J. D. *Chem. Phys. Lett.* **1981**, *80*, 37.
(18) The traditional σ–π formation is inadequate to describe the bonding in **7**, which can be rationalized in terms of off-axis overlap of tin sp^2 and p orbitals: Davidson, P. J.; Harris, D. H.; Lappert, M. F. *J. Chem. Soc., Dalton Trans.* **1976**, 2268. Fjeldberg, T.; Haaland, A.; Lappert, M. F.; Schilling, B. E. R.; Seip, R.; Thorne, A. J. *Chem. Commun.* **1982**, 1407. For a different view of the bonding in **7** see: Pauling, L. *Proc. Natl. Acad Sci. U.S.A.* **1983**, *80*, 3871.
(19) (a) Roelandt, F. F.; Van de Vondel, D. F.; Van der Kelen, G. P. *J. Organomet. Chem.* **1979**, *165*, 151. (b) Snyder, L. C.; Wasserman, Z. R. *J. Am. Chem. Soc.* **1979**, *101*, 5222. (c) Krogh-Jespersen, K. *J. Phys. Chem.* **1982**, *86*, 1492. (d) Lischka, H.; Kohler, H. *J. Chem. Phys. Lett.* **1982**, *85*, 467.
(20) (a) Tidwell, T. T. *Tetrahedron* **1979**, *34*, 1855. (b) Liebman, J. F.; Greenberg, A. *Chem. Rev.* **1976**, *76*, 311. (c) Sakurai, H.; Nakadaira, Y.; Tohita, H.; Ito, T.; Torumi, K.; Ito, H. *J. Am. Chem. Soc.* **1982**, *104*, 300. (d) Greenberg, A.; Liebman, J. F. In "Strained Organic Molecules"; Academic Press: New York, 1978; pp 108–112.
(21) One indication of greater steric hindrance in **1b** than **1a** is the generally lower reactivity of **1b** in addition reactions. In addition, the fact that two mesityl rings can be nearly coplanar with the Si=Si double bond in **1a**, but not in **1b**, suggests greater geometrical restriction in the latter compound.

Table IV. Interatomic Angles (deg) in 1b (esd's in Parentheses)

Si-Si-C(1)	123.86 (8)	C(3)-C(2)-C(7)	117.8 (2)	C(5)-C(6)-C(9)	118.1 (2)
Si-Si-C(10)	122.77 (8)	C(2)-C(3)-C(4)	122.5 (2)	Si-C(10)-C(11)	110.3 (2)
C(1)-Si-C(10)	113.2 (1)	C(3)-C(4)-C(5)	117.7 (2)	Si-C(10)-C(12)	109.6 (2)
Si-C(1)-C(2)	121.1 (2)	C(3)-C(4)-C(8)	120.8 (3)	Si-C(10)-C(13)	110.5 (2)
Si-C(1)-C(6)	120.8 (2)	C(5)-C(4)-C(8)	121.5 (3)	C(11)-C(10)-C(12)	108.7 (3)
C(2)-C(1)-C(6)	118.0 (2)	C(4)-C(5)-C(6)	122.3 (2)	C(11)-C(10)-C(13)	109.9 (3)
C(1)-C(2)-C(3)	119.7 (2)	C(1)-C(6)-C(5)	119.7 (2)	C(12)-C(10)-C(13)	107.9 (3)
C(1)-C(2)-C(7)	122.5 (2)	C(1)-C(6)-C(9)	122.1 (2)		

Recent ab initio calculations suggest that disilenes may be much more susceptible to deformation than corresponding olefins. Calculations on the ground-state structure of Si_2H_4 show a shallow potential energy surface with two local minima represented by the trans-bent and planar geometries, the trans-bent form being less than 0.5 kcal mol^{-1} more stable than the planar.[17b,19b-d] If disilenes with organic substituents behave similarly, the bond angles at silicon could easily be determined by the lattice environment. Tentatively, we attribute the differences in molecualr geometry at the Si=Si double bond in **1a** and **1b** to lattice effects.[22] If this is so, it is quite possible that the dominant conformations of **1a** and **1b** in solution are different from those found in the solid state; spectroscopic evidence[8] suggests that several conformations coexist in solutions of **1a**.

The malleability of the disilene moiety may be appreciated by comparison of **1a** with its organic analogue, tetramesitylethylene. Although the ethylene must be more strained than **1a** due to the shorter C=C double bond, it nevertheless adopts a planar conformation.[23]

The orientation of the mesityl rings relative to the disilene plane in **1b** is largely determined by steric factors. The essentially orthogonal twisting of these rings relative to the disilene framework minimizes steric repulsions between the *tert*-butyl groups and mesityl rings. On the other hand, both electronic and steric factors seem to be important in the determination of ring orientation in **1a**, in which one pair of cis-related rings are more nearly coplanar with the double bond than the other pair. We propose that electronic stabilization of ring geometry arises from conjugation of the nearly coplanar set of mesityl rings with the silicon–silicon double bond. These rings are prevented from achieving a geometry even more favorable for conjugation by severe nonbonded contacts between endo-oriented *o*-methyl groups of the mesityl rings. The nonbonded contact for these groups is 391 pm, slightly shorter than the van der Waals' distance.

Probable aryl–distance conjugation in **1a** is also indicated by its electronic absorption spectrum, which differs significantly from that for **1b**. The lowest energy band for **1a**, at 420 nm, has been asigned on the basis of considerable spectroscopic evidence as a π–π^* transition.[24] The lowest energy absorption for **1b** lies at somewhat shorter wavelength, 385 nm. The bathochromic shift for **1a** compared to **1b** is consistent with conjugative interaction between mesityl rings and the Si=Si double bond in **1a** but not in **1b**. Distortions at the double bond in **1a** may also affect the electronic absorption, but additional data will be needed for a clear appraisal of the effects of these factors.[25]

Table V. Summary of Crystal Data and Intensity Collection

	1a	1b
emperical formula	$Si_2C_{36}H_{44}\cdot C_7H_8$	$Si_2C_{26}H_{40}$
cryst dimens, mm	0.70 × 0.80 × 0.85	0.35 × 0.40 × 0.45
temp, K	188 ± 5	248 ± 5
cell parameters		
a, Å	12.064 (2)	8.968 (2)
b, Å		10.377 (2)
c, Å	52.506 (7)	7.745 (2)
α, deg		93.79 (2)
β, deg		114.19 (1)
γ, deg		98.63 (1)
space group	$I4_1/a$	$P\bar{1}$
Z	8	1
D_{calcd}, g/cm^3	1.09	1.06
abs coeff, μ, cm^{-1}	0.86	1.13
scan range		
(deg below $2\theta_{K\alpha_1}$	0.8	0.8
(deg above $2\theta_{K\alpha_2}$	0.65	0.8
scan speed, deg/min	1.5-12.0	3.0-24.0
scan type	ω	θ-2θ
2θ limits, deg	3.5-58.7	3.5-54.9
$(\sin\theta)\lambda_{max}$, Å^{-1}	0.690	0.649
unique data, theoretical	5249	2941
$F_o > 3\sigma(F_o)$	3718	2596
discrepancy indices		
R_1	0.068	0.065
R_2	0.077	0.076
goodness of fit	2.16	2.01

Experimental Section

Proton NMR spectra were recorded on a Brucker WP-200 FT spectrometer or on a Varian EM-100 spectrometer; ^{29}Si spectra were recorded on a JEOL FX-200 spectrometer and on a Varian FT-80 spectrometer. All reactions and manipulations were carried out under an atmosphere of nitrogen, and the solvents used were dried and distilled prior to use. Melting points are uncorrected.

Photolysis were carried out in a Rayonet Model RPR-100 photoreactor equipped with 254-nm lamps. Low temperatures for photolysis were maintained by the use of a quartz Dewar equipped with a liquid-nitrogen blow-off system and temperature controller.

$(Mes)_2SiCl_2$. A solution of 50.0 g of bromomesitylene (0.251 mol) in 200 mL of dry ethyl ether was added to 104 mL of 2.4 M *n*-butyllithium in hexane (0.25 mol) over a period of 1 h at room temperature. Analysis by gas chromatography (GLC) showed the formation of mesityllithium (MesLi) to be incomplete, and therefore an additional 50 mL of the *n*-butyllithium solution was added. The mixture was stirred for 1 h, and the ethyl ether was removed by distillation and replaced by 200 mL of dry benzene. To this mixture was added 14 mL of $SiCl_4$ (0.122 mol) over a period of 30 min. The resulting solution was then refluxed for 24 h and allowed to cool. At this point the reaction was complete as seen by GLC. The lithium salts were filtered, and the filtrate

(22) The lattice constraints do not appear to be particularly large. In **1a**, there are several intermolecular CH_3–CH_3 distances between 385 and 400 pm, the shortest being 378.5 ppm, slightly within the nominal van der Waals' contact distance of ~400 pm. All of the interatomic distances between the disilene and toluene molecules are outside the van der Waals' contact limit. In **1b** the intermolecular distance between two of the *tert*-butyl methyls, C(11)–C(11), is only 356.1 ppm. There are also several *tert*-butyl to *o*- or *p*-methyl distances of 383–395 pm.

(23) Blount, J. F.; Mislow, K.; Jacobus, J. *Acta Crystallogr., Sect. A* **1972**, *28A*, 512.

(24) The assignment is consistent with polarized fluorescence and resonance Raman data as well as PPP-type calculations. Details will be reported separately.[8]

(25) Long wavelength absorptions in hindered peralkyldisilenes have recently been attributed to torsional distortion about the Si–Si double bond.[2f] Pyramidal distortion that could affect the electronic absorption also seems likely in these compounds.

Table VI. Fractional Coordinates for 1a

atom	x	y	z	B_{iso},[a] Å^2
Si	0.91445 (6)	0.72362 (6)	0.14483 (1)	3.13
C(11)	0.86481 (18)	0.67042 (20)	0.11316 (4)	2.82
C(12)	0.83615 (21)	0.74136 (21)	0.09296 (4)	3.19
C(13)	0.80071 (24)	0.69696 (24)	0.06993 (5)	3.73
C(14)	0.79159 (23)	0.58435 (24)	0.06616 (5)	3.88
C(15)	0.82153 (23)	0.51441 (24)	0.08603 (5)	3.82
C(16)	0.85819 (20)	0.55528 (21)	0.10905 (5)	3.20
C(17)	0.8436 (3)	0.86668 (24)	0.09527 (7)	4.20
C(18)	0.7484 (4)	0.5372 (4)	0.04147 (7)	5.45
C(19)	0.89378 (26)	0.47347 (26)	0.12942 (6)	4.17
C(21)	0.83089 (18)	0.67936 (20)	0.17307 (4)	2.76
C(22)	0.87420 (19)	0.62267 (22)	0.19449 (4)	3.26
C(23)	0.80549 (23)	0.59936 (25)	0.21495 (5)	3.77
C(24)	0.69460 (22)	0.62927 (25)	0.21542 (5)	3.83
C(25)	0.65275 (23)	0.68269 (25)	0.19433 (5)	3.64
C(26)	0.71730 (19)	0.70884 (19)	0.17334 (4)	2.94
C(27)	0.99414 (25)	0.5880 (3)	0.19616 (6)	4.25
C(28)	0.6214 (4)	0.6046 (5)	0.23808 (7)	5.45
C(29)	0.66428 (26)	0.76993 (28)	0.15145 (6)	3.78
C(1E)	0	1/4	−0.0104 (4)	19.64
C(2)	0.0271 (18)	0.348 (4)	0.0039 (7)	13.94
C(3C)	0.0313 (8)	0.3391 (12)	0.02644 (25)	13.67
C(4)	0	1/4	0.0397 (4)	11.16
C(5A)	0	1/4	0.0621 (6)	16.57
C(B)	0.0437 (13)	0.3510 (24)	0.0545 (7)	10.69
C(D)	0	1/4	0.0124 (5)	10.32
H(13)	0.7858 (22)	0.7418 (22)	0.0577 (5)	3.8 (6)
H(15)	0.8156 (22)	0.4305 (23)	0.0847 (5)	4.7 (6)
H(17A)	0.930 (4)	0.896 (4)	0.0910 (9)	12.3 (14)
H(17B)	0.804 (3)	0.895 (3)	0.0845 (7)	7.6 (10)
H(17C)	0.850 (3)	0.889 (3)	0.1146 (8)	9.8 (11)
H(18A)	0.666 (3)	0.504 (3)	0.0436 (7)	8.1 (10)
H(18B)	0.786 (3)	0.475 (3)	0.0364 (7)	7.2 (10)
H(18C)	0.750 (3)	0.589 (3)	0.0304 (7)	6.9 (11)
H(19A)	0.8759 (28)	0.396 (3)	0.1218 (7)	7.8 (9)
H(19B)	0.8479 (25)	0.4842 (24)	0.1453 (6)	5.3 (7)
H(19C)	0.976 (3)	0.4906 (28)	0.1343 (6)	6.9 (8)
H(23)	0.8360 (20)	0.5616 (20)	0.2308 (5)	3.9 (6)
H(25)	0.5763 (23)	0.7000 (22)	0.1935 (5)	4.2 (6)
H(27A)	1.019 (3)	0.565 (3)	0.1811 (7)	8.2 (11)
H(27B)	1.049 (3)	0.665 (3)	0.2014 (7)	8.1 (10)
H(27C)	1.0108 (26)	0.5331 (26)	0.2091 (6)	5.7 (7)
H(28A)	0.6500 (29)	0.6525 (28)	0.2532 (7)	7.0 (9)
H(28B)	0.553 (4)	0.645 (3)	0.2346 (7)	9.5 (12)
H(28C)	0.631 (5)	0.556 (4)	0.2451 (11)	12.7 (21)
H(29A)	0.6583 (26)	0.7237 (26)	0.1374 (6)	5.6 (8)
H(29B)	0.5995 (26)	0.8049 (24)	0.1560 (5)	5.2 (7)
H(29C)	0.7053 (26)	0.8367 (28)	0.1464 (6)	5.9 (8)

[a] The isotropic equivalents of the anisotropic thermal motion are given for the atoms that were refined anisotropically.

was concentrated in vacuo, yielding a white crystalline solid. Subsequent recrystallization from hexane gave 19.9 g (48%) of $(Mes)_2SiCl_2$: mp 118–122 °C; ^1H NMR (C_6D_6) δ 1.99 (s, 6 H), 2.46 (s, 12 H), 6.59 (s, 4 H); MS (70 eV), m/e 336 (M^+), 321 ($M^+ - CH_3$), 217 ($M^+ - C_9H_{11}$); exact mass for $C_{18}H_{22}SiCl_2$ calcd m/e 336.0863, found m/e 336.0869.

(Mes)$SiCl_3$. Bromomesitylene (50 g, 0.251 mol) was converted to MesLi as above. The ethyl ether was removed by distillation, and the benzene solution of MesLi was transferred via cannula to an addition funnel. The solution was added dropwise to a refluxing solution of 60 mL of $SiCl_4$ (0.522 mol) in 1 L of dry benzene over a period of 2 h. The mixture was refluxed for 24 h and allowed to cool. GLC analysis showed the reaction to be complete. A workup similar to the one used in the above preparation yielded a white crystalline solid. Subsequent recrystallization from THF gave 29.6 g (48%) of $(Mes)SiCl_3$: mp 38–40 °C; ^1H NMR (C_6D_6) δ 1.94 (s, 3 H), 2.54 (s, 6 H), 6.52 (s, 2 H); MS (30 eV), m/e 252 (M^+), 217 ($M^+ - Cl$), 182 ($M^+ - Cl_2$), 133 ($M^+ - C_9H_{11}$); exact mass for $C_9H_{11}SiCl_3$ calcd m/e 251.9694, found m/e 251.9695.

(Mes)(*t*-Bu)$SiCl_2$. $(Mes)SiCl_3$ prepared as above (0.471 g, 1.86×10^{-3} mol) was dissolved in 15.0 mL of dry hexane and cooled to 0 °C with an ice/water bath. *tert*-Butyllithium (1.00 mL, 1.8 M) was syringed into the cooled solution, and the resulting mixture was allowed to warm to room temperature whereupon a white precipitate formed. After being stirred overnight, the cloudy mixture was transferred to a separatory funnel and washed once with distilled water to remove salts (the hindered dichlorosilane is inert to hydrolysis by water). The solution was dried over $MgSO_4$ and concentrated *in vacuo*, yielding 0.48 g (93%) of pure (Mes)(*t*-Bu)$SiCl_2$ as a white solid: mp 84–86 °C; ^1H NMR ($CDCl_3$) δ 1.08 (s, 9 H), 2.20 (s, 3 H), 2.55 (s, 6 H), 6.88 (s, 2 H); MS (30 eV), m/e 274 (M^+), 217 ($M^+ - C_4H_9$); exact mass for $C_{13}H_{20}SiCl_2$ calcd m/e 274.0707, found m/e 274.0710.

2,2-Dimesitylhexamethyltrisilane, 2a. A solution consisting of 23 mL (0.180 mol) of $(CH_3)_3SiCl$ and 6.8 g (0.279 mol) of Mg turnings in 98.0 mL of dry hexamethylphosphoramide (HMPA) (0.558 mol) was heated to 90 °C. Dimesityldichlorosilane (15.0 g, 0.041 mol) dissolved in 50 mL of dry tetrahydrofuran (THF) was added dropwise to the heated mixture. The colorless mixture immediately turned yellow and gradually darkened, giving a deep organe solution after 40 h of heating. After the solution had cooled, hexane was added, and the solution was filtered through glass wool to remove excess Mg. The resulting mixture was hydrolyzed with 10% HCl and the hexane layers were carefully washed with distilled water to remove any HMPA and then dried over $MgSO_4$. Concentration of the solution in vacuo yielded 15.6 g of a white powder. Subsequent recrystallization from hexane and ethanol gave 14.0 (88%) of pure **2a**: mp 169–171 °C; ^1H NMR (C_6D_6) δ 0.28 (s, 18 H), 2.10 (s, 3 H), 2.26 (s, 3 H), 6.65 (s, 2 H); MS (70

Table VII. Fractional Coordinates for 1b

atom	x	y	z	B_{iso}, [a] Å^2
Si	0.46876 (7)	0.40428 (6)	0.91906 (11)	2.94
C(1)	0.25097 (26)	0.30316 (20)	0.7989 (3)	2.69
C(2)	0.14310 (27)	0.31553 (22)	0.6113 (4)	3.12
C(3)	−0.01152 (29)	0.23039 (25)	0.5196 (4)	3.43
C(4)	−0.06461 (27)	0.13396 (22)	0.6063 (4)	3.14
C(5)	0.0396 (3)	0.12383 (24)	0.7917 (4)	3.44
C(6)	0.19523 (29)	0.20647 (23)	0.8906 (3)	3.25
C(7)	0.1869 (4)	0.4188 (4)	0.5030 (5)	4.64
C(8)	−0.2292 (4)	0.0390 (3)	0.4980 (6)	4.09
C(9)	0.2992 (5)	0.1883 (4)	1.0940 (5)	5.11
C(10)	0.62656 (27)	0.32595 (23)	0.8651 (4)	3.29
C(11)	0.7991 (3)	0.4147 (4)	0.9630 (7)	4.58
C(12)	0.5739 (4)	0.3067 (4)	0.6475 (5)	4.94
C(13)	0.6335 (4)	0.1909 (3)	0.9317 (6)	5.01
H(3)	−0.085 (4)	0.2438 (28)	0.396 (4)	4.9 (7)
H(5)	0.004 (4)	0.0595 (28)	0.859 (4)	4.8 (6)
H(7A)	0.100 (6)	0.432 (5)	0.410 (7)	10.5 (14)
H(7B)	0.246 (7)	0.494 (6)	0.569 (8)	12.3 (17)
H(7C)	0.282 (6)	0.409 (5)	0.487 (6)	9.9 (13)
H(8A)	−0.205 (4)	−0.032 (4)	0.477 (5)	6.7 (9)
H(8B)	−0.287 (6)	0.026 (4)	0.572 (6)	9.3 (12)
H(8C)	−0.303 (5)	0.085 (4)	0.408 (6)	8.7 (11)
H(9A)	0.396 (6)	0.266 (6)	1.172 (8)	12.6 (16)
H(9B)	0.333 (6)	0.113 (6)	1.114 (8)	11.6 (17)
H(9C)	0.250 (8)	0.208 (6)	1.170 (9)	14.0 (21)
H(11A)	0.796 (4)	0.503 (4)	0.917 (5)	7.5 (10)
H(11B)	0.828 (4)	0.420 (3)	1.095 (5)	5.0 (8)
H(11C)	0.874 (4)	0.368 (3)	0.936 (5)	6.0 (8)
H(12A)	0.580 (4)	0.390 (4)	0.594 (5)	6.9 (9)
H(12B)	0.459 (4)	0.241 (3)	0.573 (4)	5.4 (7)
H(12C)	0.657 (5)	0.270 (4)	0.620 (6)	8.3 (10)
H(13A)	0.663 (4)	0.201 (3)	1.064 (5)	5.2 (8)
H(13B)	0.512 (5)	0.128 (4)	0.871 (5)	7.0 (8)
H(13C)	0.718 (4)	0.154 (3)	0.910 (5)	6.7 (9)

[a] The isotropic equivalents of the anisotropic thermal motion is given for the atoms that were refined anisotropically.

eV), m/e 412 (M^+), 339 ($M^+ - Si(CH_3)_3$); exact mass for $C_{24}H_{40}Si_3$ calcd m/e 412.2427, found m/e 412.2433. Anal. Calcd for $C_{24}H_{40}Si_3$: C, 69.82; H, 9.77; Si, 20.41. Found: C, 69.74; H, 9.88; Si, 20.23.

2-*tert*-Butyl-2-mesitylhexamethyltrisilane, 2b. (Mes)(*t*-Bu)$SiCl_2$ (8.4 g, 0.031 mol) was added to a solution consisting of 8.0 mL (0.062 mol) of $(CH_3)_3SiCl$ and 2.0 g (0.012 mol) of Mg turnings in 22.0 mL (0.126 mol) of dry HMPA. The mixture was stirred and heated to 80 °C whereupon a brown color appeared. After 17 h the reaction was cooled and hydrolyzed with a 10% HCl solution. Workup similar to that for **2a** and evaporation of solvent in vacuo left a crude white solid which was shown to be pure **2b** by NMR. Subsequent recrystallization from 2:1 ethanol/THF afforded 8.8 g of **2b** (81%): ^1H NMR (C_6D_6) δ 0.36 (s, 18 H), 1.18 (s, 9 H), 2.10 (s, 3 H), 2.53 (s, 6 H), 6.89 (s, 2 H); ^{29}Si NMR ($CDCl_3$) δ −14.6, −25.7; MS (30 Ev), m/e 350 (M^+), 293 ($M^+ - C_4H_9$), 277 ($M^+ - Si(CH_3)_3$); exact mass for $C_{19}H_{38}Si_3$ calcd m/e 350.2271, found m/e 350.2281. Anal. Calcd for $C_{19}H_{38}Si_3$: C, 65.06; H, 10.92; Si, 24.02. Found: C, 63.37; H, 11.26; Si, 23.55.

Photolyses of Trisilanes 2a and 2b. A solution of 0.5 g of **2a** or **2b** in pentane was placed in a quartz photolysis tube equipped with a recrystallization chamber attached as a side arm.[26] The amount of pentane used was 40 mL for generation of **1a** and 15 mL for **1b**. The stirred solution was cooled and photolyzed. The solution turned yellow immediately, and precipitation of disilene product began within a few hours. Aliquots were withdrawn at periodic intervals, exposed to oxygen, and analyzed by GLC. Oxygen converts **1a** and **1b** quantitatively to the cyclodisiloxanes **5a** and **5b**, respectively; the amount of disilene produced was estimated from the yield of **5a** or **5b**, and hexamethyldisilane, as well as the amount of **2a** or **2b** remaining. In the case of **1a** the photolysis was carried out at −60 °C for 15 h; for **1b** a temperature of −80 °C was required for 24 h. In both cases conversion to the disilene is >95% by GLC or NMR analysis. After the photolysis was complete, pentane and hexamethyldisilane were removed in vacuo, and fresh pentane was distilled into the tube until the solid disilene redissolved. Conversion to the disilene is >95% for both **1a** and **1b**, by GLC or NMR analysis. The products in this form are suitable as starting materials for chemical reactions, but in order to obtain analytically pure disilene, the yellow solution was transferred through a frit into the sidearm and cooled to −78 °C. After precipitation the product was filtered, yielding 97 mg of **1a** (30%) and 80 mg of **1b** (27%) as air-sensitive powders. **1a**: ^1H NMR (toluene-d_8) δ 2.05 (s, 3 H), 2.43 (s, 6 H), 6.67 (s, 2 H); ^{29}Si NMR (toluene-d_8) δ +63.6. Anal. Calcd for $C_{36}H_{44}Si_2$: C, 81.12; H, 8.33; Si, 10.55. Found: C, 81.20; H, 8.42; Si, 10.67. **1b**: ^1H NMR (C_6D_6) δ 1.13 (s, 9 H), 2.13 (s, 3 H), 2.88 (s, 6 H), 6.90 (s, 2 H); ^{29}Si NMR (C_6D_6) δ +90.3; MS (30 eV), m/e 408 (M^+), 351 ($M^+ - (CH_3)_3C$). Exact mass for $C_{26}H_{40}Si_2$ calcd m/e 408.2658, found m/e 408.2671.

X-ray Data Collection. Single crystals of **1a** and **1b** were grown by slow cooling of saturated solutions in toluene to 0 °C. Those of **1a** contained one molecule of toluene per molecule of disilene. Suitably sized crystals were taken from the solution under Ar and immediately mounted on a thin glass thread with cyanoacrylate cement. A thin coat of this cement was used to seal the surface of the crystals from the Ar.

Both studies were carried out on a Syntex-Nicolet P$\bar{1}$ diffractometer with a modified LT-1 low-temperature cooling system. Unit cell parameters were obtained from least-squares refinements based on the setting angles of 60 reflections. For **1a** the space group was uniquely determined by the systematic absences in the data; for **1b** P$\bar{1}$ was assumed and confirmed by successful structure

(26) See: Fink, M. J. Ph.D. Thesis, University of Wisconsin—Madison, Aug 1983.

(27) Cromer, D. T.; Weber, J. T. "International Tables for X-ray Crystallography"; Kynoch Press: Birmingham, England, 1974; Vol. 4, pp 99–101, Table 2.2B. Stewart, R. F.; Davidson, E. R.; Simpson, W. T. *J. Chem. Phys.* **1965**, *42*, 3175.

(28) After the submission of this paper, a report on the X-ray crystal structure of another disilene derivative appeared: Masamune, S.; Murakami, S.; Snow, J. T.; Tobita, H.; Williams, D. J. *Organometallics* **1984**, *3*, 333. In the structure described in this communication, the silicon atoms and attached carbons are coplanar but the Si–Si bond is twisted by 10°. Thus this structure shares some features in common with **1a** and **1b** but is different from either.

solution and refinement. The dimensions, unit cell parameters, and other crystal data are given in Table V. Throughout data collection four standard reflections were measured every 50 reflections to monitor stability. The structures were solved by direct methods using MULTAN 78 for **1a** and MULTAN 76 for **1b**. *E* maps revealed the positions of the silicon and carbon atoms. Subsequent electron density difference maps revealed overlapping positions for the disordered toluene solvate. Further electron density difference maps revealed the nonsolvent hydrogen atoms. In the final cycles of refinement all non-hydrogen atoms were assumed to vibrate anisotropically and all hydrogen atoms were assumed to vibrate isotropically. The final R values ($R_1 = \sum||F_o| - |F_c||/\sum|F_o|$; $R_2 = [\sum w(|F_o| - |F_c|)^2/\sum w(F_o)^2]^{1/2}$) are also included in Table V. The final atomic coordinates for **1a** and **1b** are listed in Tables VI and VII, respectively.

Acknowledgment. Research was supported by the Air Force Office of Scientific Research, Air Force Systems Command, USAF, under Grant No. AFOSR-82-0067 and the National Science Foundation (Grant CHE80-00256). The United States government is authorized to reproduce and distribute reprints for governmental purposes notwithstanding any copyright notation thereon.

Registry No. **1a**, 80785-72-4; **1b**, 88526-23-2; **2a**, 79184-72-8; **2b**, 88526-27-6; **3a**, 79184-71-7; **3b**, 89486-28-2; **4a**, 88957-30-6; **4b**, 89486-29-3; **5a**, 84537-22-4; **5b**, 89486-30-6; MesLi, 5806-59-7; $(Mes)_2SiCl_2$, 5599-27-9; $(Mes)SiCl_3$, 17902-75-9; $(Mes)(t\text{-}Bu)SiCl_2$, 89486-31-7; bromomesitylene, 576-83-0.

Supplementary Material Available: Final anisotropic thermal parameters and listings of $10|F_o|$ and $10|F_c|$ for **1a** and **1b** (31 pages). Ordering information is given on any current masthead page.

Communications

Synthesis and Structural Characterization of $[Fe_4(\mu_3\text{-}S)_3(\mu_3\text{-}S_2)Cp_4][MoOCl_4(thf)]$. A New Fe–S Cluster with Different Modes of Coordination at the Iron Sites

N. Dupre,[†] H. M. J. Hendriks,[†] J. Jordanov,*[†] J. Gaillard,[‡] and P. Auric[§]

Département de Recherche Fondamentale
Centre d'Etudes Nucléaires de Grenoble
85 X, F.38041 Grenoble Cedex, France

Received November 22, 1983

Summary: Reaction of $Fe_4S_6(Cp)_4$ with $MoOCl_3(thf)_2$ generates $[Fe_4(\mu_3\text{-}S)_3(\mu_3\text{-}S_2)Cp_4][MoOCl_4(thf)]$. Structural data show that the cation contains a distorted Fe_4S_5 core with a triply bridging S_2^{2-} ligand and with one Fe having expanded its ligation to four sulfurs. EPR and Mössbauer studies lead to the core formal electronic description [3 Fe^{III}, 1 Fe^{II}].

Recent findings show that natural[1-3] Fe–S clusters are not confined to the well-studied species having planar 2Fe–2S and cubane-type [4Fe–4S] core units.[4]

This has triggered a series of synthetic efforts to obtain heretofore unknown polynuclear Fe/S geometries, which have resulted in the isolation and structural characterization of $[Et_4N][Fe_3S(O\text{-}xyl)_3]$,[5] $[Et_4N]_3[Fe_3S_4(SPh)_4]$,[6] $Fe_4S_6(Cp)_4$,[7] $[Fe_6S_8(PEt_3)_6][BPh_4]_2$,[8] and $[Et_4N][Fe_6S_9(SEt)_2]$.[6,9]

Moreover, [4Fe–4S] clusters of a novel type have been identified at the "P" sites of nitrogenase,[10] with unique and so far unexplained spectral and magnetic properties. It has been suggested[10,11] that the protein could achieve this by use of non-thiolate ligands at the Fe sites, or geometric distortion of the 4Fe–4S core from tetrahedral geometry, or expansion to pentacoordination for the Fe atoms.

While investigating the reactivity of Mo compounds vs. $Fe_4S_6Cp_4$, we isolated a solid of composition $[Fe_4S_5Cp_4][MoOCl_4(thf)]$ (I). We report here the synthesis and structural characterization of this interesting cluster, where a S_2^{2-} ligand bonded to three Fe sites is present and one of the Fe's has expanded its ligation to four S and one Cp.

Reaction of $Fe_4S_6Cp_4$[7] with $MoOCl_3(thf)_2$[12] in dichloromethane (CH_2Cl_2) at room temperature under argon gives instantenously complex I,[13] presumably by reaction of Mo with one of the disulfide groups, followed by S abstraction.

$$Fe_4S_6(Cp)_4 + 2MoOCl_3(thf)_2 \rightarrow [Fe_4S_5Cp_4][Mo^{V}OCl_4(thf)] + (1/n)[Mo^{VI}OSCl_2]_n$$

Its infrared spectrum displays ν(Mo=O) = 957 (m) cm^{-1}, ν(Mo—Cl) = 330 (sh), 305 (s) cm^{-1}, ν(S—S) = 525 (w) cm^{-1}, and ν(Fe—S) = 466 (m) cm^{-1}.[14] The UV–visible spectrum

[†] Laboratoires de Chimie (LA CNRS No. 321).
[‡] Laboratoire de Résonance Magnétique.
[§] Laboratoire d'Interactions Hyperfines.

(1) (a) Stout, C. D.; Ghosh, D.; Pattabhi, V.; Robbins, A. H. *J. Biol. Chem.* **1980**, *255*, 1797. (b) Ghosh, D.; Furey, W., Jr.; O'Donnell, S.; Stout, C. D. *Ibid.* **1981**, *256*, 4185.
(2) (a) Hatchikian, E. C.; Bruschi, M. *Biochem. Biophys. Res. Commun.* **1979**, *86*, 725. (b) Hatchikian, E. C.; Bruschi, M. *Biochim. Biophys. Acta* **1981**, *634*, 41.
(3) Adams, M. W. W.; Mortenson, L. E.; Chen, J. S. *Biochim. Biophys. Acta* **1981**, *594*, 105.
(4) (a) Holm, R. H. *Acc. Chem. Res.* **1977**, *10*, 427. (b) Ibers, J. A.; Holm, R. H. *Science (Washington, D.C.)* **1980**, *209*, 223. (c) Chu, C. T. W.; Lo, F. Y. K.; Dahl, L. F. *J. Am. Chem. Soc.* **1982**, *104*, 3409.
(5) Henkel, G.; Tremel, W.; Krebs, B. *Angew. Chem., Int. Ed. Engl.* **1981**, *20*, 1033.
(6) Hagen, K. S.; Watson, A. D.; Holm, R. H. *J. Am. Chem. Soc.* **1983**, *105*, 3905.
(7) Kubas, G. J.; Vergamini, P. J. *Inorg. Chem.* **1981**, *20*, 2667.
(8) Cecconi, F.; Ghilardi, C. A.; Midollini, S. *J. Chem. Soc., Chem. Commun.* **1981**, 640.
(9) Henkel, G.; Strasdeit, H.; Krebs, B. *Angew. Chem., Int. Ed. Engl.* **1982**, *21*, 201.
(10) Münck, E.; Rhodes, H.; Orme-Johnson, W. H.; Davis, L. C.; Brill, W. J.; Shah, V. K. *Biochim. Biophys. Acta* **1975**, *400*, 32.
(11) Averill, B. A. *Struct. Bonding (Berlin)* **1983**, *53*, 59.
(12) Kepert, D. L.; Mandyczewsky, R. *J. Chem. Soc. A* **1968**, 530.
(13) In an argon-filled glovebox, 0.348 g (0.5 mmol) of $Fe_4S_6Cp_4$ in 100 mL of CH_2Cl_2 is added to a solution (20 mL) of 0.357 mg (1 mmol) of $MoOCl_3(thf)_2$ also in CH_2Cl_2, and the resulting mixture is stirred for 15 min. The brown solid is filtered, washed with CH_2Cl_2, and dried under vacuum. Complex I is extracted with acetonitrile, whereby a brown residue is left, which is insoluble in most organic solvents and tentatively formulated as $MoOSCl_2$ of polymeric structure (diamagnetic; ν(Mo–O–Mo) = 700 (m) cm^{-1}, ν(Mo–S–Mo) = 455 (m) cm^{-1}, ν(Mo–Cl) = 330 (s) cm^{-1}. Complex I is soluble, but decomposes in chlorinated solvents and is recrystallized from CH_3CN–THF–hexane (35% yield). Elemental analyses were performed by Le Service Central d'Analyse, CNRS, Vernaison. Satisfactory analytical data were obtained for C, H, S, Cl, Fe, Mo.

0276-7333/84/2303-0800$01.50/0